THEORY AND EXPERIMENTS ON THE HYPERSONIC SOURCE FLOW OVER LONG, SLENDER BODIES IN A CONICAL NOZZLE

M. Yasuhara, S. Watanabe, H. Mitome and M. Ikeda
Department of Aeronautical Engineering,
Nagoya University, Nagoya, Japan

Abstract

First, inviscid, non-linear, quasi-similarity theory is applied to a long body in a hypersonic source flow, and second, linearized theory for a pointed body is treated by the method of source distribution. These source flow results show large decrease in the surface pressure distribution compared with the parallel ones in the rear part of the body, if the distance from the nose to the body surface normalized by the source-nose distance, increases beyond about 0.1. Third, it is shown that there exists one-to-one correspondence between source flow problem and parallel one in the slender body theory when the ratio γ of specific heats of gas is equal to 2. This result, combined with the empirical assumption that the pressure coefficient is insensitive to the difference of the value of γ, is useful to give an estimation of the pressure distribution over a power-law body in a parallel flow, if the pressure over the modified body in a source flow is obtained theoretically or experimentally, provided that the viscous effect is ignored. Last, pressure distributions along power-law bodies measured in the conical nozzle of a hypersonic shock tunnel are compared with the non-linear theory, and also the source-parallel conversion result, giving essentially good coincidences.

I. Theory

I-A. Quasi-similarity theory

Studies of supersonic source flow past bodies have been of current interests, because these simulate the flow in a divergent section of a hypersonic wind-tunnel, or the one in a central core of the low density free jet, etc.. Many of theoretical analyses use Newtonian theory or its modification as given by Hall[1], Brun and Guibergia[2] etc., while method of characteristics is used by Baradell and Bertram[3] and Süveges[4] etc.. Also, Savage[5] and Gorgui[6] applied a direct perturbation method to the source flow past wedges or cones, and presented the first order results, which, however, is useful for rather narrow region behind the nose. Yasuhara and Watanabe[7] applied the similarity expansion for power-law bodies in the special case of the ratio of specific heats of 2.0.

The present part deals with the hypersonic source flow past a long slender body by the quasi-similarity approximation.

A-1. Source flow, shock condition, and basic equations

In an inviscid, steady, supersonic flow expanding cylindrically (β=1) or spherically (β=1), the flow quantities at a distance r from the effective source, can be obtained from the simple nozzle flow relations. Denote T_1 is the temperature, p_1 the pressure, ρ_1 the density, u_1 the radial velocity, M_1 the local Mach number in the free stream at radial distance r from the source. Also suffixes "o" and "*" denote quanities at the stagnation and the imaginary sonic point, respectively. The log-log plot of flow quantities against $(r/r^*)^\beta \equiv (s)^\beta$ for γ=1.4 are shown in Fig.1. For moderately high values of M_1 compared to unity, flow quantities are approximated as follows:

$$p_1/p_N = s^{-\beta\gamma\varepsilon}\ ,\quad \rho_1/\rho_N = s^{-\beta\varepsilon}\ , \tag{1}$$

$$u_1/u_N = s^{\beta(\varepsilon-1)}\ ,\quad M_1/M_N = s^{\beta\lambda}\ ,$$

where

$$s \equiv r/r_N\ ,\quad \varepsilon \equiv M_N^2/(M_N^2-1)\ ,$$

$$\lambda \equiv \frac{\gamma+1}{2}\cdot\varepsilon - 1\ .$$

In the above, suffix "N" denotes exact quantities at the nose of the body $r=r_N$ (s=1), θ=0. Eq. (1) gives accurate values around $r=r_N$ because the above equations express tangential lines to each curve at (r_N/r^*) in Fig.1. The larger the value of M_N, the wider the range of applicability of Eq.(1) is.

Now, as shown in Fig.2, an axisymmetric hypersonic source flow past a slender body with a closed nose, is considered, in which the shock wave is assumed to be attached to the nose of the body at $r=r_N$. The cylindrical or spherical polar coordinates (r,θ) are used. In this system, the position of the shock and body surface at r are expressed, respectively, by:

$$\theta = \theta_w(r) \quad , \qquad \theta = \theta_b(r), \tag{2}$$

$$\theta_w = 0 \text{ and } \theta_b = 0 \text{ at } r = r_N.$$

where the subscript "w" and "b" denote quantities just behind the shock wave and along the body surface.
With these notations, the shock angle σ between the radial ray and the shock line is given by:

$$\tan\sigma = rd\theta_w/dr = sd\theta_w/ds \equiv s\theta_w', \tag{3}$$

where "'" denotes the differentiation with respect to s. If $\sigma<<1$, then the quantities just behind the shock wave are given by:

$$p_w = \frac{2\rho_1 u_1^2\sigma^2}{(\gamma+1)}\left\{1 - \frac{\gamma-1}{2\gamma}(M_1\sigma)^{-2}\right\} \quad ,$$

$$\rho_w = \rho_1 \frac{(\gamma+1)(M_1\sigma)^2}{2+(\gamma-1)(M_1\sigma)^2} \quad ,$$

$$u_w = u_1 - \frac{2u_1\sigma^2}{(\gamma+1)}\frac{(M_1\sigma)^2 - 1}{(M_1\sigma)^2} \doteq u_1 \quad , \tag{4}$$

$$v_w = \frac{2u_1\sigma}{(\gamma+1)}\frac{(M_1\sigma)^2 - 1}{(M_1\sigma)^2} \quad ,$$

provided that $M_1\sigma>1$, where u and v are the radial and θ-wise velocity components, respectively. If θ in the disturbed field is very small compared to unity, the basic equations of motion are given by:

$$\frac{1}{r^\beta}\frac{\partial}{\partial r}(\rho u r^\beta) + \frac{1}{r\theta^{\beta-1}}\frac{\partial}{\partial\theta}(\rho v\theta^{\beta-1}) = 0,$$

$$u\frac{\partial u}{\partial r} + \frac{v}{r}\frac{\partial u}{\partial\theta} - \frac{v^2}{r} = -\frac{1}{\rho}\frac{\partial p}{\partial r} \quad ,$$

$$u\frac{\partial v}{\partial r} + \frac{v}{r}\frac{\partial v}{\partial\theta} + \frac{uv}{r} = -\frac{1}{\rho r}\frac{\partial p}{\partial\theta} \quad , \tag{5}$$

$$u\frac{\partial}{\partial r}(p/\rho^\gamma) + \frac{v}{r}\frac{\partial}{\partial\theta}(p/\rho^\gamma) = 0.$$

A-2. Quasi-similarity theory

Referring to the shock condition Eq. (4), the independent variables (r,θ) and flow variables p,ρ,u and v are transformed into (ξ,η) and P,R,U and V as follows,

$$\xi = M_1\sigma \quad , \quad \eta = \theta/\theta_w \quad , \tag{6}$$

$$p = \rho_1 u_1^2\sigma^2 P(\xi,\eta), \quad \rho = \rho_1 R(\xi,\eta) \quad ,$$

$$u = u_1 U(\xi,\eta), \quad v = u_1\sigma V(\xi,\eta). \tag{7}$$

Then, after neglecting smaller quantities of $0(\theta^2)$ compared to unity, Eq. (5) is transformed into:

$$(RV)_\eta - \eta(RU)_\eta + (\beta-1)RV/\eta = -\nu\xi(RU)_\xi,$$

$$\beta(\varepsilon-1)\omega U^2 + (V-\eta U)U_\eta = -\nu\xi UU_\xi,$$

$$\left[\{1 - \beta(\gamma-1)\varepsilon/2\}\omega + \nu\right]RUV + (V-\eta U)RV_\eta + P_\eta = -\nu\xi URV_\xi, \tag{8}$$

$$2\nu PUR + (V-\eta U)(RP_\eta - \gamma PR_\eta) = -\nu\xi(URP_\xi - \gamma UPR_\xi),$$

where subscripts "η" and "ξ" denote partial differentiations with respect to η and ξ respectively, and:

$$\xi \equiv M_1\sigma = M_N\theta_w' S^{\beta\lambda+1} \quad ,$$

$$\nu \equiv \theta_w\xi'/(\theta_w'\xi) = (1+\beta\lambda)\omega+\mu, \tag{9}$$

$$\omega \equiv \theta_w/(s\theta_w'), \quad \mu \equiv \theta_w\theta_w''/\theta_w'^2 \quad .$$

Also the shock condition Eq. (4) at $\eta=1$ $(\theta=\theta_w)$, is transformed into:

$$P_w \equiv P(\xi,1) = \frac{2(2\gamma\xi^2-\gamma+1)}{(\gamma+1)\ 2\gamma\xi^2} \quad ,$$

$$R_w \equiv R(\xi,1) = \frac{(\gamma+1)\xi^2}{2+(\gamma-1)\xi^2}$$

$$U_w \equiv U(\xi,1) = 1, \tag{10}$$

$$V_w \equiv V(\xi,1) = \frac{2(\xi^2-1)}{(\gamma+1)\xi^2} \quad .$$

The other boundary condition at the body surface is given by the tangency of the stream-line and the velocity there, that is:

$$(v/u)_b = s\theta_b' \ , \text{ or } V_b/U_b = \theta_b'/\theta_w' \ . \quad (11)$$

The similarity solution exists when P, R, U and V, including their boundary values at the shock and the body surface, are functions of η alone. These conditions are satisfied when ω, ν and ξ given by Eq.(9) are kept constants. At the same time, the following condition must be satisfied:

$$\theta_b/\theta_w = \eta_b = \text{const.}. \quad (12)$$

Formally, these conditions are satisfied when $\theta_w \propto s^{-\beta\lambda}$, which, however, is unrealistic in the present problem, because the condition of the closed nose of the body and the attached shock wave ($\theta_w=0$ at s=1) can not be satisfied. The similarity condition for which $\xi^2 >> 1$ is the same as shown by Yasuhara[7].

In general, the similarity conditions can not always be satisfied, and the local similarity approximation is tried here. If all variables along the shock wave and the body surface vary sufficiently slowly with s, then ξ, ω and ν in Eq.(8) are assumed to take on their local values at each s. Further, following to Oshima's quasi-similarity assumption[8], ξ-derivatives in the form Q_ξ/Q in Eq.(8) is evaluated at the shock, $(Q_w)_\xi/Q_w$, that is:

$$\frac{P_\xi}{P} = \frac{2(\gamma-1)}{\xi(2\gamma\xi^2-\gamma+1)}, \quad \frac{R_\xi}{R} = \frac{4}{\xi\{(\gamma-1)\xi^2+2\}} \quad (13)$$

$$\frac{U_\xi}{U} = 0., \quad \frac{V_\xi}{V} = \frac{2}{\xi(\xi^2-1)}.$$

Use of Eq.(13) in the right-hand terms of Eq.(8) makes the solution more accurate even for values of ξ not very large compared to unity.

In these manners, Eq.(8) can be regarded as the ordinary differential equations with ω, ν and ξ as parameters, and thus integrable from the shock to the body surface. The condition Eq.(11) requires some consideration. If $\theta_b(s) \propto \theta_w(s)$, then η_b is independent of s. However, in general, η_b is a function of s through parameters ξ, ω and μ. Thus, using the relation:

$$\theta_w = \theta_b/\eta_b, \quad (14)$$

Eq.(11) is expressed in terms of $\theta_b(s)$ and $\eta_b(s)$ as

$$\left(\frac{V}{U}\right)_b = \frac{\theta_b'}{\theta_w'} = \frac{\eta_b}{1-(\eta_b'/\eta_b)(\theta_b/\theta_b')} \ . \quad (15)$$

Unless the term η_b'/η_b is known apriori, the right-hand side of Eq.(15) can not be evaluated as the boundary condition. To express this term as a function of s, an iteration is necessary. With the aid of Eq.(14), ω, μ and ξ are expressed in terms of s, θ_b, η_b and their derivatives with respect to s, that is η_b, θ_b' and θ_b''. Now, at the nose of the body s=1, θ_b equals to zero and therefore $\omega=0$ and μ takes some constant value there. Also, assuming several values of $\eta_b(s=1)=\eta_{0i}$, for example, $\eta_{0i}=0.85$, 0.90 etc., the corresponding values of $\xi=\xi_{0i}$ at s=1, are calculated. Then the right-hand sides of Eq.(13) can be calculated. Introducing the above relations into the right-hand side of Eq.(8), the system of ordinary equations for R,U,V and P can be integrated for each set of (η_{0i},ξ_{0i}) from η=1 down to η_0 where V-ηU=0 holds. The calculated values of η_0 are compared with the assumed values of η_{0i}, and by interpolating and further iterating the procedure, the value of η_0, as well as all values at s=1 are determined. Next, to integrate the equations for s larger than 1, the range of s to be calculated is divided into k parts., and the value of η_b, as a function of s, is approximated by the continuation of inclined line segments as follows:

$$\eta_{b,j} = \eta_{b,j-1} + \alpha_j(s_j-s_{j-1}) + \beta_j(s_j-s_{j-1})^2/2,$$

$$j=j,\ldots\ldots,\ k,$$

$$\eta_{b,j}' = d\eta_{b,j}/ds = \alpha_j + \beta_j(s_j-s_{j-1}),$$

$$\eta_{b,j}'' = \beta_j,$$

with $\eta_b = \eta_0$ at s = 1.
After determining all values at $s=s_{j-1}$, values at $s=s_j$ can be integrated as follows: by assuming several values of α_j and β_j, the values of $\eta_{b,j}$, $\eta_{b,j}'$, $\eta_{b,j}''$ and ξ_j can be calculated, from which the corresponging values of ω, μ and ξ are obtained. Then with the help of Eq.(13), Eq.(8) can be integrated from η=1 down to $\eta=\eta_{b,j}$ where Eq.(15) holds. Then deduced values of $\eta_{b,j}$ are compared with the assumed values of $\eta_{b,j}$, and by interpolating and further iterating the procedure, the value of $\eta_{b,j}$ and α_j, β_j as well as all values at $s=s_j$ are determined. In the following computations, η_b'' is assumed to be zero as an approximation.

A-3. Power-law body

In the present section, solutions of the source flow past slender power-law bodies with conical asymtote is treated. The equation of the body considered is given by:

$$\theta_b = \delta(1-\frac{1}{s})^m , \qquad \delta<<1 \qquad (16)$$

where m=1 corresponds to a circular cone. With the above θ_b introduced into Eq.(15), we have:

$$V_b/(\eta U)_b = 1/\{1-\eta_b' s(s-1)/(m\eta_b)\} \qquad (17)$$

It is easily shown that at s=1, Eq.(17), ω, μ and ξ reduce to:

$$(V/\eta U)_b = 1, \quad \omega = 0, \quad \mu = (m-1)/m,$$

$$\xi = M_N\delta/\eta_b, \quad \text{for} \quad m = 1,$$

$$\xi = \infty, \qquad \text{for } m < 1.$$

The value of ξ at s=1 for m=1 can not be given apriori unless the value of η_b there is known, and must be obtained by an iteration. To accomplish this, first assuming several values of ξ_i, Eq.(8) is integrated from the shock to the body surface, under the condition that $\mu=\omega=0$, and then, from the obtained values of $\eta_{b0}(\xi i)$, the correct value of ξ is interpolated so as the relation $\xi=M_N\delta/\eta_b$ is satisfied. In the case when m<1, the value of ξ at s=1 can be assumed as infinity.

For the value of s greater than unity, the successive approximation described in the preceding section is performed.

Several numerical results for m=1 and 3/4 with γ=1.4 are shown as follows:

1) Circular cone

The results of cone (m=1) with semivertex angle of 15° in a point source flow (β=2), are shown in Fig.3 to 6. Figs.3 and 4 show the values of η_b and ξ as functions of s for nose Mach number of M_N=7.5 and ∞, Fig.5 shows the pressure function P as the function of η for several values of s in the case M_N=7.5. From the figures it can be seen that P does not vary so much in between the shock (η=1) and the body surface ($\eta=\eta_b$) for each s. Also η_b slightly diminishes as s increases from 1. The pressure coefficient C_{pl} along the cone surface referred to the free stream pressure p_1 is given by:

$$C_{pl} \equiv \frac{p_b-p_1}{\rho_N u_N^2/2} \qquad (18)$$

$$= \frac{2(\tan^2\alpha)P_b}{\eta_b^2 s^{6-2\varepsilon}}\{1-s(s-1)\eta_b'/\eta_b\}^2 - \frac{2}{\gamma M_N^2 s^{2\gamma\varepsilon}}$$

Therefore in the case of $M_N=\infty$, if P_b and η_b are taken as their mean values with η_b' neglected, then p_b is proportional to s^{-4}. Figs.6a and 6b show the pressure pressure distributions along the cone surface when M_N=7.5, and ∞, showing the large variation of C_{pl} as s increases. Such a large variation of pressure along the surface demonstrates that the power series expansion of flow quantities in powers of (s-1) is inadequate beyound s>1.1.

For comparison, the Newtonian pressure distribution corresponding to $M_N=\infty$ is calculated as follows. In this case, the pressure on the surface at radial distance r is given by:

$$p_b = \rho_1 u_1^2 \sin^2\sigma$$

where $\sigma=\alpha-\theta_w$, $r\sin\sigma=r_N\sin\alpha$. Therefore when $\alpha,\theta_w<<1$,

$$p_b/(\tfrac{1}{2}\rho_N u_N^2) = 2\sin^2\sigma/s^2 = 2\alpha^2/s^4.$$

That is, the pressure is proportional to s^{-4}. Fig.6b shows also the result for $M_N=\infty$ calculated by Gorgui for γ=1.4, and the one calculated by the Newtonian approximation. The present results essentially coincide with Gorgui's one near the nose region(s=1~1.1). The present result and the Newtonian one for $M_N=\infty$ show essentially a good comparison for a wide renge of s (s=1~2).

2) 3/4 power-law body

This corresponds to the body shown in Eq.(16) with m=3/4, which has the 3/4 power-law body near the nose, and approaches a cone asymptotically as s increases. Calculating procedure is almost the same as 1) except the nose point s=1. Figs.3 and 4 show the values of η_b and ξ as functions of s for M_N=7.5. Fig.7 shows the pressure distribution along the surface.

I-B. Linearized theory

In hypersonic flows, most of the important problems require non-isentropic, non-linear teatments. However, if the body is very slender in the sense that the effective hypersonic surface parameter $\bar{\chi}$ (the product of the local free stream mach number M_1 and the angle ε of the body surface with respect to the local free stream direction), is smaller than unity, the flow field can be assumed as isentropic with good accuracy, and the supersonic potential flow theory is applicable. Further, the perturbed equation can be linearized when $\bar{\chi}$ is moderately smaller than unity.

In the present section, the source flow over a very slender body of revolution is discussed by a linearized perturbation theory.

In the polar coordinates system (r,θ), the basic equations of the axisymmetric flow over a pointed body of

revolution, are given by Eq.(5). It is assumed that $\chi=M_1\varepsilon$ is smaller than unity, which implies that θ in the disturbed flow field is very small everywhere. Because the flow is assumed to be isentropic, there exists a velocity potential Φ defined by:

$$u = \frac{\partial\Phi}{\partial r} \equiv \Phi_r, \quad v = \frac{1}{r}\frac{\partial\Phi}{\partial\theta} \equiv \frac{1}{r}\Phi_\theta \tag{19}$$

Then the gas dynamic equation is derived from Eq.(5) and (19) as follows:

$$\Phi_{rr}(1-\frac{\Phi_r^2}{a^2}) + \frac{\Phi_{\theta\theta}}{r^2}(1-\frac{\Phi_\theta^2}{r^2a^2}) - \frac{2\Phi_r\Phi_\theta\Phi_{\theta r}}{r^2a^2}$$

$$+ \frac{\Phi_r}{r}(2+\frac{\Phi_\theta^2}{r^2a^2}) + \frac{\Phi_\theta\cot\theta}{r^2} = 0. \tag{20}$$

Here, the square a^2 of the local sound speed takes the form:

$$a^2 \equiv (\gamma-1)(H-\frac{1}{2}\Phi_r^2-\frac{\Phi_\theta^2}{2r^2}),$$

where

$$H \equiv \frac{\gamma}{\gamma-1}\frac{p}{\rho} + \frac{1}{2}(u^2+v^2) = \text{const.}.$$

Φ is divided into free stream and perturbation potentials ϕ_0 and ϕ_1 by:

$$\Phi(r,\theta) = \phi_0(r) + \phi_1(r,\theta),$$

$$u = \Phi_r = \phi_{0r} + \phi_{1r}, \quad v = \frac{1}{r}\Phi_\theta = \frac{1}{r}\phi_{1\theta} \tag{21}$$

It is assumed that the body is very slender and the perturbed velocity components are very small compared with the free stream velocity such that:

$$\phi_{0r} >> \phi_{1r}, \quad \frac{1}{r}\phi_{1\theta}.$$

Then after higher order terms than $0(v/a)$ are neglected, Eq.(20) is reduced to:

$$(1-M_1^2)\phi_{0rr} + \frac{2}{r}\phi_{0r} = 0,$$

$$(1-M_1)\phi_{1rr} + \frac{2M_1^2\{2+(\gamma-1)M_1^2\}}{r(1-M_1^2)}\phi_{1r}$$

$$+ \frac{\phi_{1\theta\theta}}{r^2} + \frac{2}{r}\phi_{1r} + \frac{\phi_{1\theta}}{\theta r^2} = 0, \tag{22}$$

where M_1 can be approximated by:

$$M_1 = M_N s^{\gamma-1}, \text{ with } M_N >> 1. \tag{23}$$

If the non-dimensional variables z and ω are introduced by:

$$z \equiv s^{-(\gamma-1)/(\gamma-1)}, \quad \omega \equiv M_N\theta \tag{24}$$

then with the aid of Eq.(23), the perturbation equation Eq.(22) for ϕ_1, is transformed into:

$$\phi_{1zz} + \frac{k}{z}\phi_{1z} - \phi_{1\omega\omega} - \frac{1}{\omega}\phi_{1\omega} = 0, \tag{25}$$

where

$$k \equiv (2-\gamma)/(\gamma-1).$$

Further, when ψ is introduced by:

$$\phi_1 = \psi/Z, \tag{26}$$

then Eq.(25) is transformed into:

$$\psi_{zz} + \frac{2-k}{z}\psi_z - \psi_{\omega\omega} - \frac{1}{\omega}\psi_\omega = 0. \tag{27}$$

Eq.(25) is solved by Yasuhara[10] et al. for $\gamma=2(k=0)$ and $\gamma=1.5(k=1)$, using the menthod of source distribution. While if $\gamma=4/3$, then k=2 and Eq.(27) has the same form as Eq.(25) for k=0. The general solution of ϕ_1 for a pointed body with $\gamma=4/3$ can be expressed as follows:

$$\phi_1 = -\frac{1}{\eta}\int_{\eta+\omega}^{3} \frac{h(\eta_1)d\eta_1}{\sqrt{(\eta_1-\eta)^2-\omega^2}} = -\frac{1}{\eta}\int_0^{\cosh^{-1}(3-\eta)/\omega} h(\eta+\omega\cosh\sigma)d\sigma$$

$$\eta = 3/s^{1/3}, \tag{28}$$

where $h(\eta_1)$ denotes the source distribution function along the body axis, to be determined from the surface condition. The boundary condition along the body surface gives that:

$$\{\Phi_\theta/(r\Phi_r)\}_b = (v/u)_b = rd\theta_b/dr,$$

or

$$(\phi_{1\omega})_b = -\frac{9u_N r_N}{M_N^2\eta^2}\frac{d\omega_b}{d\eta}, \tag{29}$$

where u_N is the free-stream velocity at the nose of the body.

The pressure coefficient C_p referred

to the free-stream pressure p_N at the nose is given by:

$$C_p \equiv (p_b-p_N)/(\rho_N u_N^2/2) \tag{30}$$

The perturbed pressure coefficient C_{pl} referred to the local free-stream pressure p_1 is, within the present approximation, expressed by:

$$C_{pl} = (p_b-p_1)/(\rho_N u_N^2/2) = -\frac{1}{s^2}\{2\frac{\phi_{1r}}{u_N}+(\frac{\phi_{1\theta}}{ru_N})^2\}, \tag{31}$$

Practical methods of solution for $\gamma=4/3$ are almost the same as given in Ref.10.

Fig.8 shows the calculated pressure distribution along the very slender cone with the semi-vertex angle $\alpha=4°$ when $M_N=7.5$. Also shown in the figure are the results when $\gamma=2.0$ and 1.5 obtained in Ref.10, respectively. All these curves are close each other, and this shows that the pressure distribution expressed in the form C_{pl} is, practically not sensitive to the difference in the value of γ. However, if it is expressed in the form C_p, then appreciable differences can be seen as shown in Ref.10.

I-c. Equivalency between source and parallel flows for $\gamma=2$.

As shown shortly in Ref.7, there is some one-to-one correspondence relation between source flow problem and parallel one in inviscid, hypersonic small disturbance theory, provided that $\gamma=2$. According to this relation, the problem for the power-law cone in a hypersonic source flow expressed by the polar coordinates $\theta_b=\delta(1-1/s)^m$, is equivalent to the one for the power-law body in the parallel flow expressed by the cylindrical coordinates $y_b/L=\delta(x/L)^m$. If the problem for the parallel flow with the free stream Mach number of M_N is solved, the pressure coefficient $C_p(x/L; M_N,\gamma)$ is expressed in terms of x/L. Then, the corresponding pressure coefficient C_{pl} referred to the free stream pressure p_1 in the source flow with the free stream nose Mach number of M_N, can be related to C_p through the simple conversion relation:

$$C_{pl}(s;M_N,\gamma)=C_p(1-1/s;M_N,\gamma)/s^4=C_p/s^4,$$

provided that $\gamma=2$. In the above, x/L in the expression of C_p for the parallel flow is replaced by $1-1/s$.

Now, although the above value of $\gamma(=2)$ is different from that for actual gases, if the coefficient C_p in the parallel flow is not much sensitive to such a difference of γ, as shown in Lees and Kubota's analyses (Ref.11, 12), then C_{pl} for the source flow with γ_1 can be obtained from $C_p(x/L; M_N, \gamma)$, by simply dividing it by s^4, in which x/L should be replaced by $1-1/s$, that is:

$$C_{pl}(s;M_N,\gamma_1)=C_p(1-1/s;M_N,\gamma)/s^4.$$

In the above conversion, it is assumed that the term C_p on the right-hand side is also insensitive to the difference of γ_1 in the source flow problem.

In Figs.6 and 7, the pressure distributions along the cone and the 3/4 power-law nosed cone, calculated by applying the above equivalence relation are shown. The equivalence results and the quasi-similarity results show good comparisons as a whole.

II. Experiments

II-A Shock tunnel and test conditions.

Experiments on hypersonic source flows over long slender cone, 3/4 power-law body and hemisphere cylinder, etc., are performed in a conical nozzle of the shock tunnel at the Nagoya University. The Mach number M_N of the free stream at the nose of bodies are fixed to 7.5, and surface pressures are measured and compared with the above theories. The details of the tunnel are shown in Ref.13, and therefore shortly described here. The tunnel consists of the driver tube (200mmϕx5302mm), the driven tube (100mmϕ x9998mm), the conical nozzle (10° semi-vertex angle with throat and exit diameters of 13mmϕ and 300mmϕ), and the dump tank (1450mmϕ x 6125mm). The initial pressures of the driver, driven tube and the dump tank are fixed to 41.0kg/cm^2, 1.03kg/cm^2, and 0.1 torr, respectively.

The configuration of the nozzle and test section is shown in Fig.9. Air is used as the working gas.

The models employed are shown in Fig. 10. Each pressure hole on a model surface (1.5 or 2.0mmϕ) is connected to a piezo resistance type pressure gauge directly, or through a 1.5mmϕ lead-pipe. The pressue p_0 in the stagnation region just upstream of the nozzle is measured by the Kistler gange. The impact pressure probe is used to measure the distribution of the impact pressure p_t along the nozzle axis. Fig.11 shows an example of time traces of p_0 and p_t. The traces show very similar patterns, with the first transient duration having pressure rise and slight fall, followed by

the second time interval with an essentially constant pressure, which is regarded as the testing time range, and then further pressure fall after about 70ms from the onset of pulse. From the measured values of p_0 and p_t in the testing time range at several axial positions x, the distribution of the free stream Mach number M_1 and the corresponding effective area ratio $A/A^*=(r/r^*)^2$ or its square root r/r^* (r is the radial distance from the effective source, and * denotes the effective throat condition), are computed, and r/r^* is plotted against x in Ref.14. This $x-(r/r^*)$ relation was shown to be straight approximately, which means that the flow in the present conical nozzle can be assumed to be a source flow.

II-B Distributions of surface pressures.

Although experimental pressure distribution on the cone against $s=r/r_N$ was reported in Ref.14, this is again shown as well as the new results on the 3/4 power-law nosed cone. The pressure coefficient C_{p1} is referred to the local free stream pressure p_1, that is:

$$C_{p1} = \frac{p_b - p_1}{\rho_N u_N^2/2} ,$$

Figs.6a and 7 show the experimental pressure coefficients C_{p1} against s for the cone and the 3/4 power-law body in the source flow with the free stream Mach number M_N at the nose of 7.5, respectively. Also shown in these figures are inviscid, theoretical resuts obtained by the present quasi-similarity approximation for $\gamma=1.4$, and also ones obtained by applying the extended parallel-source equivalence for power-law bodies. Comparisons between theories and experiments give essentially good correspondence except some discrepancies caused by the viscous effects, which were not considered in the present theories, and by experimental errors, as well as by errors included in the present empirical assumption.

Conclusions

First, the inviscid, hypersonic quasi-similarity theory is applied to a long body in a source flow, and practical calculations for a cone and a 3/4 power-law body are given. Second, the linearized theory for a very slender pointed body is treated by the method of source distribudion, and the results for a very slender cone in the source flow with $\gamma=2$, 1.5 and 4/3 are compared, showing close coincidences each other. Third, the one-to-one correspondence between source flow and parallel one for power-law-bodies when $\gamma=2$, is extendedly applied to the case for any γ, under the empirical assumption that the pressure coefficient in the flow is insensitive to the difference of γ. Last, experiments on the source flow over a long cone and a 3/4 power-law body in the conical nozzle of a hypersonic shock tunnel are described, and the measured pressure distributions are compared with the above theories, giving essentially good coincidences except discrepancies caused by the viscous effects (which are not considered in theories) and experimental errors.

Acknowledgment

The present work was partly supported by the scientific funds of the Ministry of Education, and the numerical computations were performed by FACOM 230-60 at the Computation Center, Nagoya University.

References

(1) Hall, J.G.: Effects of ambient nonuniformities in flow over hypersonic test bodies, Cornell Aeronautical Labo., Rep. 128, 1963.

(2) Brun, R. et Guibergia, J.P.: Influence de la sphéricite d'dun écoulement libre hypersonique sur la distribution de la pression et du flux de chaleur á la surface de corps de révolution élancés, Jouranl de M'ecanique, Vol.6, No.1, 1967.

(3) Baradell, D.L., and Bertram, M.H.: The blunt flat plate in hypersonic flow, NASA TN D-408, 1960.

(4) Süveges, F.: Ebene Profile in Paralleler und Quellförmiger Überschallanströmung, Dissertation, TH Universität Karlsruhe, 1968.

(5) Savage, S.B.: Effects of a source-type hypersonic free stream on the flow field about an axisymmetric cone, Aeron. Quarterly, Vol.17, May, 1966.

(6) Gorgui, M.A.: The hypersonic source flow past wedges and cones, Aeron. Quarterly, Vol.22, Nov., 1971.

(7) Yasuhara, M. and Watanabe, S.: Inviscid hypersonic source flow over slender power-law bodies, Aeron. Quarterly, Vol.26, Aug., 1975.

(8) Yasuhara, M.: Hypersonic self-similarity of barrel shock in source type free jets, AIAA, Vol.4, June, 1966

(9) Oshima, K.: Blast waves produced by exploding wire, Aeron. Res. Institute, University of Tokyo, Rep. 358, July, 1960.

(10) Yasuhara, M., Mitome, H. and Nakao.F.: Linearized theory of axisymmetric hypersonic source flow past bodies of revolution, J. Fluid Mech., Vol.73, pt.1, 1976.

(11) Kubota, T.: Inviscid hypersonic flow over blunt-nosed slender bodies, GALCIT, No.417, 1957.
(12) Lees, L. and Kubota, T.: Inviscid hypersonic flow over blunt-nosed slender bodies, J. Aeron. Sci., Vol.24, March, 1957.
(13) Uchida, S., Kuwabara, K. and Furuhashi, K.: An investigation on the flow through a hypersonic nozzle in shock-gun tunnel, Memo. Faculty of Engineering, Nagoya Univ., Vol.22, Nov., 1970.
(14) Yasuhara, M., Kuwabara, K. and Watanabe. S.: Shock tunnel experiments on hypersonic source flow past slender bodies, 10th International Shock Tube Sympo., 1975.

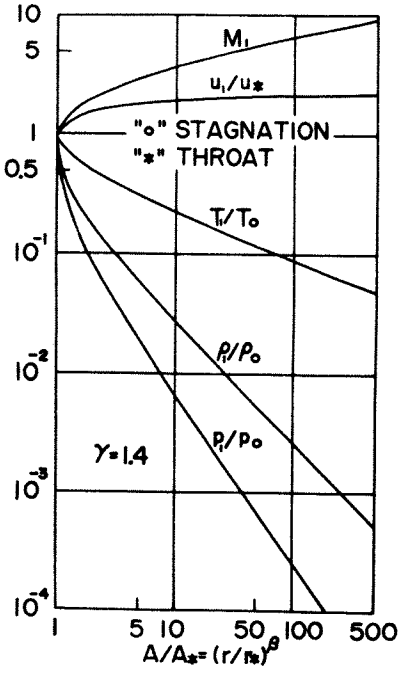

Fig.1. Flow variables versus area ratio for the uniform source flow.

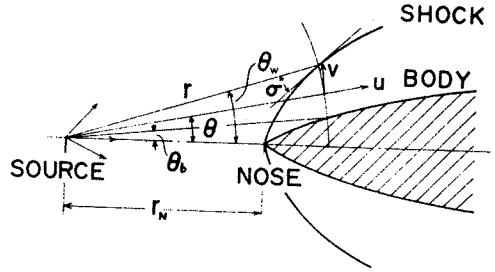

Fig.2. Flow and body geometry in the uniform source flow.

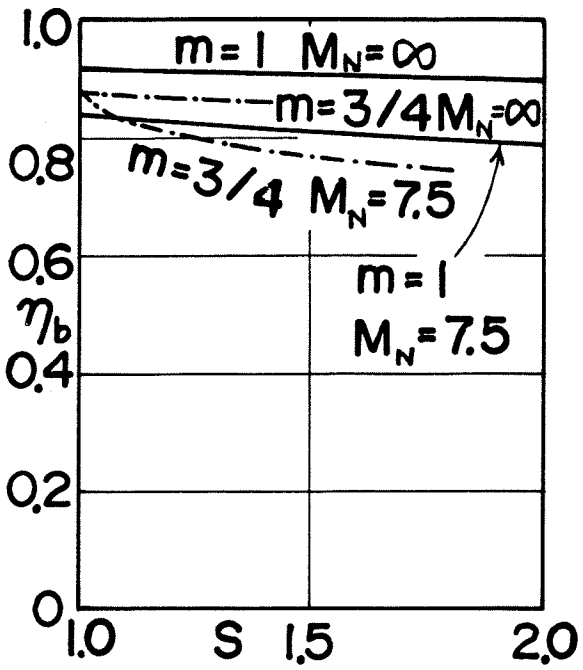

Fig.3. η_b-s relations of the quasi-similarity results for the cone (m=1) with δ=0.2679, and 3/4 power-law body (m=3/4) with δ=0.1981. M_N=0.75 and ∞, γ=1.4, β=2.

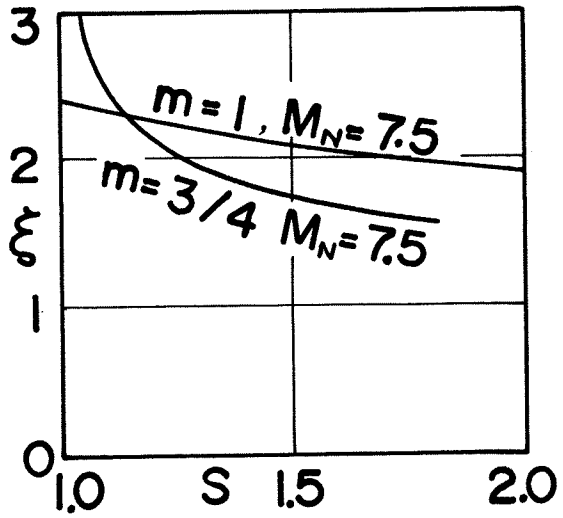

Fif.4. ξ - s relations of the quasi-similarity results for the cone (m=1) with δ=0.2679, and 3/4 power-law body (m=3/4) with δ=0.1981. M_N=7.5, γ=1.4, β=2.

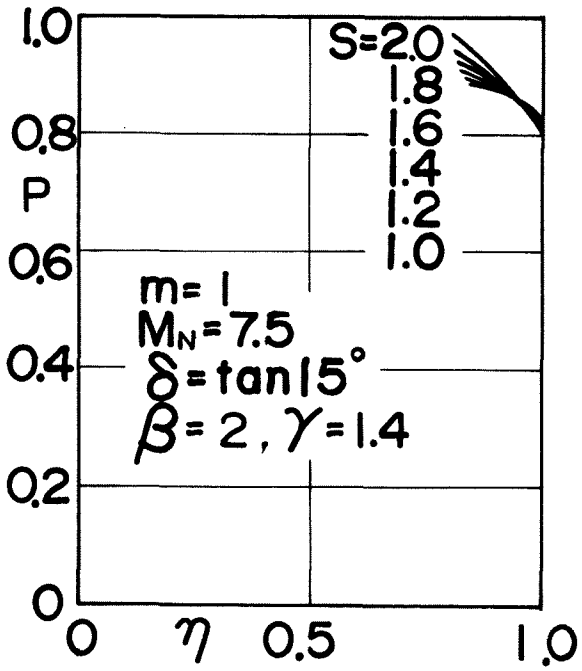

Fig.5. Pressure function P against η of the quasi-similarity results for the cone(m=1) with δ=tan15°=0.2679 at several s.

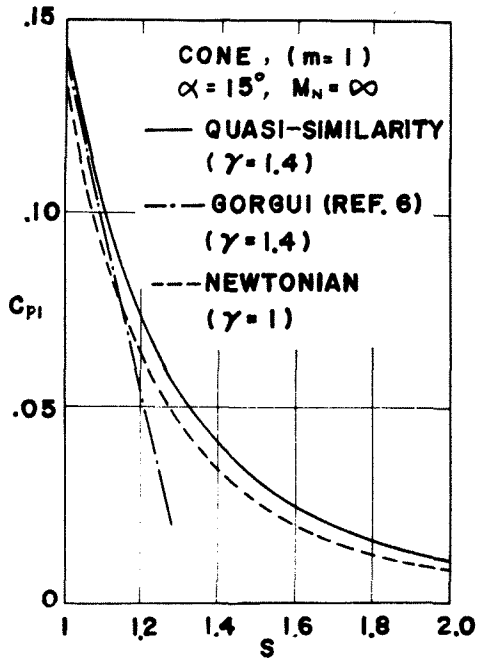

Fig.6-b. Theoretical pressure distribution c_{pl} against s for the cone(m=1) with δ=0.2679 ,M_N= ∞, β=2.

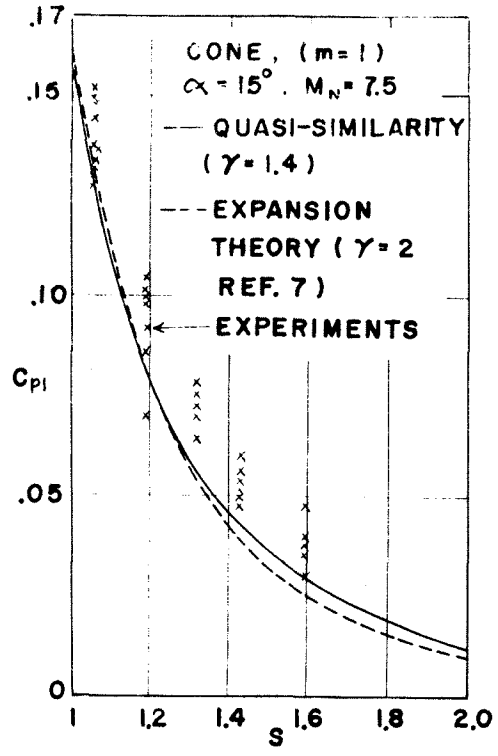

Fig.6-a. Theoretical and experimental pressure distribution c_{pl} against s for the cone, M_N=7.5. Expansion theory assumes extended source-parallel correspondence.

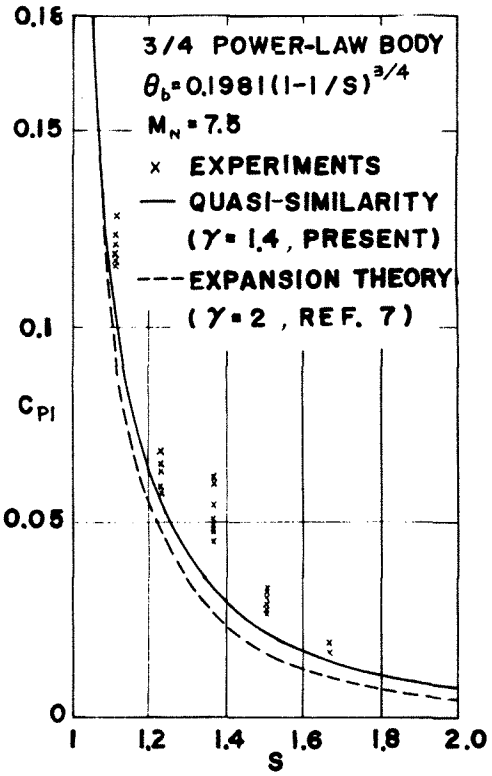

Fig.7. Theoretical and experimental pressure distribution c_{pl} against s for the 3/4 -power-law body. Expansion theory assumes extended source-parallel correspondence.

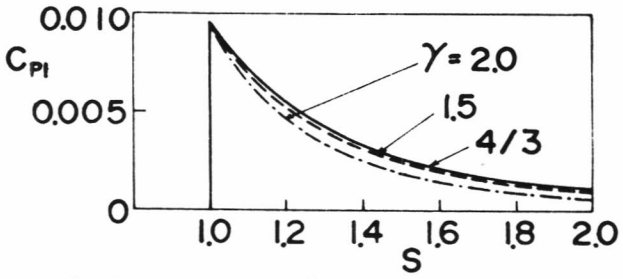

Fig.8-a. Pressure distribution c_{pl} referred to the free stream pressure p_1 against s for the very slender cone(m=1) with δ=tan4°=0.06993, M_N=7.5,β=2. Linearized theory.

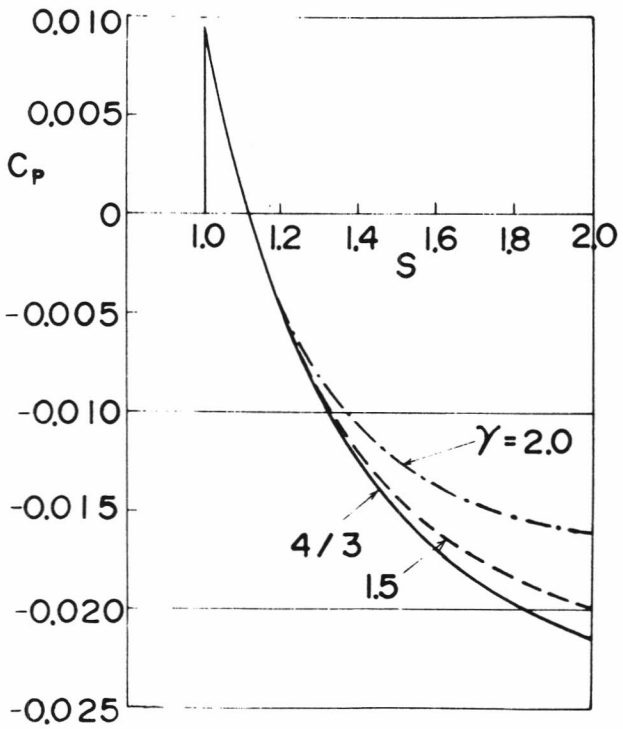

Fig.8-b. Pressure distribution c_p referred to the free stream nose pressure p_N against s , at the same flow and body conditions with Fig.8-a.

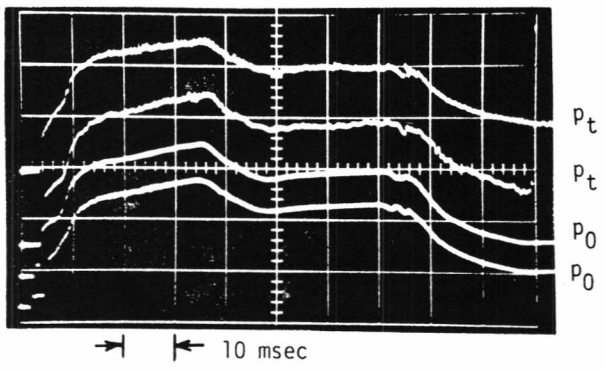

Fig.11-a. Total(p_t) and stagnation(p_o) pressure traces, by Kistler gauges.

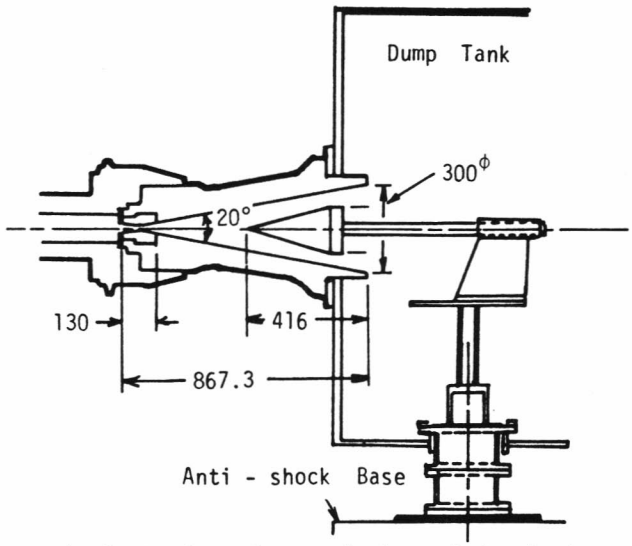

Fig.9. Nozzle and test chamber of the shock tunnel. Unit=mm.

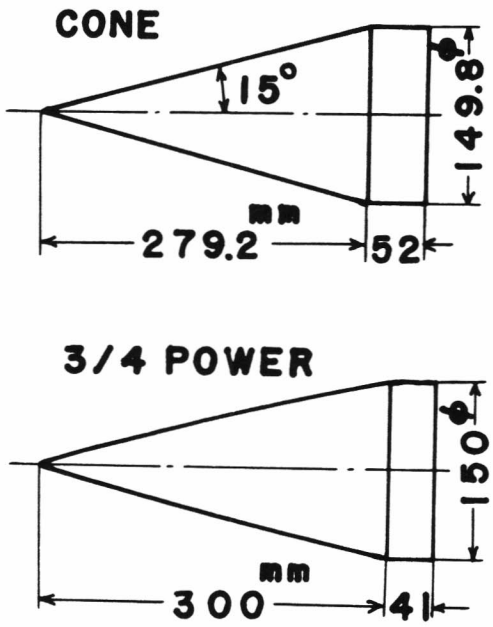

Fig.10. Experimental models. Cone(m=1) δ=0.2679 and 3/4 power-law body(m=3/4) δ=0.1981, with r_N=435 mm. Unit=mm.

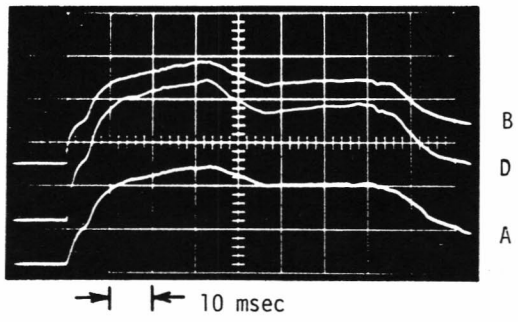

Fig.11-b. Surface(p_b) pressure traces for 3/4 power-law body, by Piezo resistance gauge.